GNSS Vertical Dilution of Precision Reduction using Terrestrial Signals of Opportunity

Joshua J. Morales, Joe J. Khalife, and Zaher M. Kassas
University of California, Riverside

BIOGRAPHIES

Joshua J. Morales is pursuing a Ph.D. from the Department of Electrical and Computer Engineering at The University of California, Riverside. He received a B.S. in Electrical Engineering with High Honors from The University of California, Riverside. His research interests include estimation, navigation, computer vision, autonomous vehicles, and intelligent transportation systems.

Joe J. Khalifeh is a Ph.D. student at The University of California, Riverside. He received a B.E. in electrical engineering and an M.S. in computer engineering from the Lebanese American University (LAU). From 2012 to 2015, he was a research assistant at LAU. His research interests include navigation, autonomous vehicles, and intelligent transportation systems.

Zaher (Zak) M. Kassas is an assistant professor at The University of California, Riverside. He received a B.E. in Electrical Engineering from The Lebanese American University, an M.S. in Electrical and Computer Engineering from The Ohio State University, and an M.S.E. in Aerospace Engineering and a Ph.D. in Electrical and Computer Engineering from The University of Texas at Austin. From 2004 through 2010 he was a research and development engineer with the LabVIEW Control Design and Dynamical Systems Simulation Group at National Instruments Corp. His research interests include estimation, navigation, autonomous vehicles, and intelligent transportation systems.

ABSTRACT

Reducing the vertical dilution of precision (VDOP) of a global navigation satellite system (GNSS) position solution by exploiting terrestrial signals of opportunity (SOPs) is considered. A receiver is assumed to make pseudorange observations on multiple GNSS satellite vehicles (SVs) and multiple terrestrial SOPs and to fuse these observations through an estimator. This paper studies GNSS VDOP reduction by adding a varying number of cellular SOPs, which are inherently at low elevation angles. It is demonstrated numerically and experimentally that adding SOP observables is more effective to reduce VDOP over adding GNSS SV observables.

I. INTRODUCTION

Global navigation satellite system (GNSS) position solutions suffer from a high vertical dilution of precision (VDOP) due to lack of satellite vehicle (SV) angle diversity. Signals of opportunity (SOPs) have been recently considered to enable navigation whenever GNSS signals become inaccessible or untrustworthy [1–3]. Terrestrial SOPs are abundant and are available at varying geometric configurations, making them an attractive supplement to GNSS for reducing VDOP.

Common metrics used to assess the quality of the spatial geometry of GNSS SVs are the parameters of the geometric dilution of precision (GDOP); namely, horizontal dilution of precision (HDOP), time dilution of precision (TDOP), and VDOP [4]. Several methods have been investigated for selecting the best GNSS SV configuration to improve the navigation solution by minimizing the GDOP [5–7]. While the navigation solution is always improved when additional observables from GNSS SVs are used, the solution's VDOP is generally of worse quality than the HDOP [8]. GPS augmentation with LocataLites, which are terrestrial transmitters that transmit GPS-like signals, have been shown to reduce VDOP [9]. However, this requires installation of additional proprietary infrastructure. This paper studies VDOP reduction by exploiting terrestrial SOPs, particularly cellular code division multiple access (CDMA) signals, which have inherently low elevation angles and are free to use.

In GNSS-based navigation, the states of the SVs are readily available. For SOPs, however, even though the position states may be known *a priori*, the clock error states are dynamic; hence, must be continuously estimated. The states of SOPs can be made available through one or more receivers in the navigating receivers vicinity [10, 11]. In this paper, the estimates of such SOPs are exploited and the VDOP reduction is evaluated.

The remainder of this paper is organized as follows. Section II formulates the GNSS+SOP-based navigation solution and corresponding GDOP parameters. Section III discusses the relationship between VDOP and observation elevation angles. Section IV presents simulation results for using a varying number of GNSS SVs and SOPs. Section V presents experimental results using cellular CDMA SOPs. Concluding remarks are given in Section VI.

II. PROBLEM FORMULATION

Consider an environment comprising a receiver, M GNSS SVs, and N terrestrial SOPs. Each SOP will be assumed

Preprint of the 2016 ION ITM Conference
Monterey, CA, January 25–28, 2016

to emanate from a spatially-stationary transmitter, and its state vector will consist of its position states $\boldsymbol{r}_{\mathsf{sop}_n} \triangleq \left[x_{\mathsf{sop}_n},\, y_{\mathsf{sop}_n},\, z_{\mathsf{sop}_n}\right]^{\mathsf{T}}$ and clock error states $c\,\boldsymbol{x}_{\mathrm{clk,sop_n}} \triangleq c\left[\delta t_{\mathsf{sop}_n},\, \dot{\delta t}_{\mathsf{sop}_n}\right]$, where c is the speed of light, $\delta t_{\mathsf{sop}_n}$ is the clock bias, and $\dot{\delta t}_{\mathsf{sop}_n}$ is the clock drift [12], where $n = 1, \ldots, N$.

The receiver draws pseudorange observations from the GNSS SVs, denoted $\{z_{\mathrm{sv_m}}\}_{m=1}^{M}$, and from the SOPs, denoted $\left\{z_{\mathsf{sop}_n}\right\}_{n=1}^{N}$. These observations are fused through an estimator whose role is to estimate the state vector of the receiver $\boldsymbol{x}_r = \left[\boldsymbol{r}_r^{\mathsf{T}},\, c\delta t_r\right]^{\mathsf{T}}$, where $\boldsymbol{r}_r \triangleq [x_r,\, y_r,\, z_r]^{\mathsf{T}}$ and δt_r are the position and clock bias of the receiver, respectively. The pseudorange observation made by the receiver on the m^{th} GNSS SV, after compensating for ionospheric and tropospheric delays, is related to the receiver states by

$$z'_{\mathrm{sv}_m} = \|\boldsymbol{r}_r - \boldsymbol{r}_{\mathrm{sv}_m}\|_2 + \, c \cdot [\delta t_r - \delta t_{\mathrm{sv}_m}] + v_{\mathrm{sv}_m},$$

where, $z'_{\mathrm{sv}_m} \triangleq z_{\mathrm{sv}_m} - \delta t_{\mathsf{iono}} - \delta t_{\mathsf{tropo}}$; $\boldsymbol{r}_{\mathrm{sv}_m}$ and δt_{sv_m} are the position and clock bias states of the m^{th} GNSS SV, respectively; δt_{iono} and $\delta t_{\mathsf{tropo}}$ are the ionospheric and tropospheric delays, respectively; and $v_{\mathrm{sv_m}}$ is the observation noise, which is modeled as a zero-mean Gaussian random variable with variance $\sigma^2_{\mathrm{sv_m}}$. The pseudorange observation made by the receiver on the n^{th} SOP, after mild approximations discussed in [12], is related to the receiver states by

$$z_{\mathsf{sop}_n} = \|\boldsymbol{r}_r - \boldsymbol{r}_{\mathsf{sop}_n}\|_2 + \, c \cdot \left[\delta t_r - \delta t_{\mathsf{sop}_n}\right] + v_{\mathsf{sop}_n},$$

where v_{sop_n} is the observation noise, which is modeled as a zero-mean Gaussian random variable with variance $\sigma^2_{\mathsf{sop}_n}$.

The measurement residual computed by the estimator has a first-order approximation of its Taylor series expansion about an estimate of the receiver's state vector $\hat{\boldsymbol{x}}_r$ given by

$$\boldsymbol{\Delta z} = \mathbf{H}\,\boldsymbol{\Delta x}_r + \boldsymbol{v},$$

where $\boldsymbol{\Delta z} \triangleq \boldsymbol{z} - \hat{\boldsymbol{z}}$, i.e., the difference between the observation vector $\boldsymbol{z} \triangleq \left[\, z'_{\mathrm{sv}_1}, \ldots, z'_{\mathrm{sv}_M}, z_{\mathsf{sop}_1}, \ldots, z_{\mathsf{sop}_N} \,\right]^{\mathsf{T}}$ and its estimate $\hat{\boldsymbol{z}}$; $\boldsymbol{\Delta x} \triangleq \boldsymbol{x}_r - \hat{\boldsymbol{x}}_r$, i.e., the difference between the receivers's state vector $\boldsymbol{x}_r$ and its estimate $\hat{\boldsymbol{x}}_r$; $\boldsymbol{v} \triangleq \left[\, v_{\mathrm{sv}_1}, \ldots, v_{\mathrm{sv}_M}, v_{\mathsf{sop}_1}, \ldots, v_{\mathsf{sop}_N} \,\right]^{\mathsf{T}}$; and $\mathbf{H}$ is the Jacobain matrix evaluated at the estimate $\hat{\boldsymbol{x}}_r$. Without loss of generality, assume an East, North, UP (ENU) coordinate frame to be centered at $\hat{\boldsymbol{x}}_r$. Then, the Jacobian in this ENU frame can be expressed as

$$\widehat{\mathbf{H}} = \left[\widehat{\mathbf{H}}_{\mathrm{sv}}^{\mathsf{T}},\, \widehat{\mathbf{H}}_{\mathsf{sop}}^{\mathsf{T}}\right]^{\mathsf{T}},$$

where

$$\widehat{\mathbf{H}}_{\mathrm{sv}} = \begin{bmatrix} \mathsf{c}(el_{\mathrm{sv}_1})\mathsf{s}(az_{\mathrm{sv}_1}) & \mathsf{c}(el_{\mathrm{sv}_1})\mathsf{c}(az_{\mathrm{sv}_1}) & \mathsf{s}(el_{\mathrm{sv}_1}) & 1 \\ \vdots & \vdots & \vdots & \vdots \\ \mathsf{c}(el_{\mathrm{sv}_M})\mathsf{s}(az_{\mathrm{sv}_M}) & \mathsf{c}(el_{\mathrm{sv}_M})\mathsf{c}(az_{\mathrm{sv}_M}) & \mathsf{s}(el_{\mathrm{sv}_M}) & 1 \end{bmatrix}$$

and

$$\widehat{\mathbf{H}}_{\mathsf{sop}} = \begin{bmatrix} \mathsf{c}(el_{\mathsf{sop}_1})\mathsf{s}(az_{\mathsf{sop}_1}) & \mathsf{c}(el_{\mathsf{sop}_1})\mathsf{c}(az_{\mathsf{sop}_1}) & \mathsf{s}(el_{\mathsf{sop}_1}) & 1 \\ \vdots & \vdots & \vdots & \vdots \\ \mathsf{c}(el_{\mathsf{sop}_N})\mathsf{s}(az_{\mathsf{sop}_N}) & \mathsf{c}(el_{\mathsf{sop}_N})\mathsf{c}(az_{\mathsf{sop}_N}) & \mathsf{s}(el_{\mathsf{sop}_N}) & 1 \end{bmatrix},$$

where $\mathsf{c}(\cdot)$ and $\mathsf{s}(\cdot)$ are the cosine and sine functions, respectively, el_{sv_m} and az_{sv_m} are the elevation and azimuth angles, respectively, of the m^{th} GNSS SV, and el_{sop_n} and az_{sop_n} are the elevation and azimuth angles, respectively, of the n^{th} terrestrial SOP as observed from the receiver. To simplify the discussion, assume that the observation noise is independent and identically distributed, i.e., $\mathrm{cov}(\boldsymbol{v}) = \sigma^2\mathbf{I}$, then, the weighted least-squares estimate $\hat{\boldsymbol{x}}_r$ and associated estimation error covariance $\mathbf{P}_{\tilde{\boldsymbol{x}}_r\tilde{\boldsymbol{x}}_r}$ are given by

$$\hat{\boldsymbol{x}}_r = \left(\widehat{\mathbf{H}}^{\mathsf{T}}\widehat{\mathbf{H}}\right)^{-1}\widehat{\mathbf{H}}^{\mathsf{T}}\boldsymbol{z}, \qquad \mathbf{P}_{\tilde{\boldsymbol{x}}_r\tilde{\boldsymbol{x}}_r} = \sigma^2\left(\widehat{\mathbf{H}}^{\mathsf{T}}\widehat{\mathbf{H}}\right)^{-1}.$$

The matrix $\widehat{\mathbf{G}} \triangleq \left(\widehat{\mathbf{H}}^{\mathsf{T}}\widehat{\mathbf{H}}\right)^{-1}$ is completely determined by the receiver-to-SV and receiver-to-SOP geometry. Hence, the quality of the estimate depends on this geometry and the pseudorange observation noise variance. The diagonal elements of $\widehat{\mathbf{G}}$, denoted $\hat{g}_{ii}$, are the parameters of the dilution of precision (DOP) factors:

$$\begin{aligned} \text{GDOP} &\triangleq \sqrt{\mathrm{tr}\left[\widehat{\mathbf{G}}\right]} \\ \text{HDOP} &\triangleq \sqrt{\hat{g}_{11} + \hat{g}_{22}} \\ \text{VDOP} &\triangleq \sqrt{\hat{g}_{33}}. \end{aligned}$$

Therefore, the DOP values are directly related to the estimation error covariance; hence, the more favorable the geometry, the lower the DOP values [13]. If the observation noise was not independent and identically distributed, the weighted DOP factors must be used [14].

The following sections illustrate the VDOP reduction by incorporating additional GNSS SV observations versus additional SOP observations.

III. VDOP REDUCTION VIA SOPs

With the exception of GNSS receivers mounted on high-flying and space vehicles, all GNSS SVs are typically above the receiver [13], i.e., the elevation angles in $\widehat{\mathbf{H}}_{\mathrm{sv}}$ are theoretically limited between $0° \leq el_{\mathrm{sv}_m} \leq 90°$. GNSS receivers typically restrict the lowest elevation angle to some elevation mask, $el_{\mathsf{sv,min}}$, so to ignore GNSS SV signals that are heavily degraded due to the ionosphere, the troposphere, and multipath. As a consequence, GNSS SV observables lack elevation angle diversity and the VDOP of a GNSS-based navigation solution is degraded. For ground vehicles, $el_{\mathsf{sv,min}}$ is typically between 10° and 20°. These elevation angle masks also apply to low flying aircrafts,

such as small unmanned aircraft systems (UASs), whose flight altitudes are limited to 500ft (approximately 152m) by the Federal Aviation Administration (FAA) [15].

In GNSS + SOP-based navigation, the elevation angle span may effectively double, specifically $-90° \leq el_{\text{sop}_n} \leq 90°$. For ground vehicles, useful observations can be made on terrestrial SOPs that reside at elevation angles of $el_{\text{sop}_n} = 0°$. For aerial vehicles, terrestrial SOPs can reside at elevation angle as low as $el_{\text{sop}_n} = -90°$, e.g., if the vehicle is flying directly above the SOP transmitter.

To illustrate the VDOP reduction by incorporating additional GNSS SV observations versus additional SOP observations, an additional observation at el_{new} is introduced, and the resulting VDOP(el_{new}) is evaluated. To this end, M SV azimuth and elevation angles were computed using GPS ephemeris files accessed from the Yucaipa, California station via Garner GPS Archive [16], which are tabulated in Table I. For each set of GPS SVs, the azimuth angle of an additional observation was chosen according to $A_{\text{new}} \sim U(0°, 359°)$. The corresponding VDOP for introducing an additional measurement at a sweeping elevation angle $-90° \leq el_{\text{new}} \leq 90°$ are plotted in Fig. 1 (a)-(d) for $M = 4, \ldots, 7$, respectively.

The following can be concluded from these plots. First, while the VDOP is always improved by introducing an additional measurement, the improvement of adding an SOP measurement is much more significant than adding an additional GPS SV measurement. Second, for elevation angles inherent only to terrestrial SOPs, i.e., $-90° \leq el_{\text{sop}_n} \leq 0°$, the VDOP is monotonically decreasing for decreasing elevation angles.

TABLE I
SV AZIMUTH AND ELEVATION ANGLES (DEGREES)

	$M=4$		$M=5$		$M=6$		$M=7$	
(m)	az_{sv_m}	el_{sv_m}	az_{sv_m}	el_{sv_m}	az_{sv_m}	el_{sv_m}	az_{sv_m}	el_{sv_m}
1	185	79	189	66	46	40	61	21
2	52	60	73	69	101	58	57	49
3	326	52	320	41	173	59	174	30
4	242	47	56	27	185	38	179	66
5	-	-	261	51	278	67	269	31
6	-	-	-	-	314	41	218	56
7	-	-	-	-	-	-	339	62

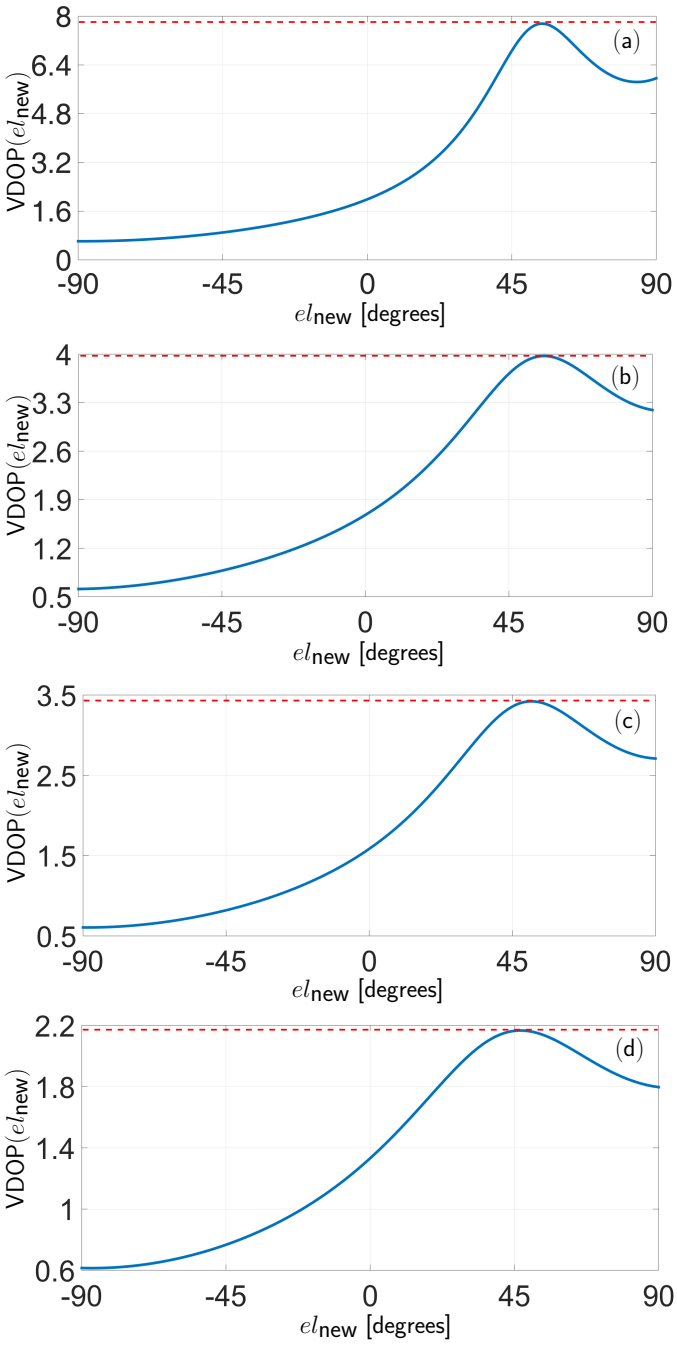

Fig. 1. A receiver has access to M GPS SVs from Table I. Plots (a)-(d) show the VDOP for each GPS SV configuration before adding an additional measurement (red dotted line) and the resulting VDOP(el_{new}) for adding an additional measurement (blue curve) at an elevation angle $-90 \leq el_{\text{new}} \leq 90$ for $M = 4, \ldots, 7$, respectively.

IV. SIMULATION RESULTS

This section presents simulation results demonstrating the potential of exploiting cellular CDMA SOPs for VDOP reduction. To compare the VDOP of a GNSS only navigation solution with a GNSS + SOP navigation solution, a receiver position expressed in an Earth-Centered-Earth-Fixed (ECEF) coordinate frame was set to $\boldsymbol{r}_r \equiv (10^6) \cdot [-2.431171, -4.696750, 3.553778]^{\mathsf{T}}$. The elevation and azimuth angles of the GPS SV constellation above the receiver over a twenty-four hour-period was computed using GPS SV ephemeris files from the Garner GPS Archive.

The elevation mask was set to $el_{\mathsf{sv,min}} \equiv 20°$. The azimuth and elevation angles of three SOPs, which were calculated from surveyed terrestrial cellular CDMA tower positions in the receivers vicinity, were set to $\boldsymbol{az}_{\mathsf{sop}} \equiv [42.4°, 113.4°, 230.3°]^{\mathsf{T}}$ and $\boldsymbol{el}_{\mathsf{sop}} \equiv [3.53°, 1.98°, 0.95°]^{\mathsf{T}}$. The resulting VDOP, HDOP, GDOP, and associated number of available GPS SVs for a twenty-four hour period starting from midnight, September 1$^{\mathsf{st}}$, 2015, are plotted in Fig. 5. These results were consistent for different receiver locations and corresponding GPS SV configurations.

The following can be concluded from these plots. First, the resulting VDOP using GPS + N SOPs, for $N \geq 1$, is always less than the resulting VDOP using GPS alone. Second, using GPS + N SOPs, for $N \geq 1$ prevents large spikes in VDOP when the number of GPS SVs drops. Third, using GPS + N SOPs, for $N \geq 1$ also reduces both HDOP and GDOP.

V. EXPERIMENTAL RESULTS

A field experiment was conducted using software defined receivers (SDRs) to demonstrate the reduction of VDOP obtained from including SOP pseudoranges alongside GPS pseudoranges for estimating the states of a receiver. To this end, two antennas were mounted on a vehicle to acquire and track: (i) multiple GPS signals and (ii) three cellular base transceiver stations (BTSs) whose signals were modulated through CDMA. The GPS and cellular signals were simultaneously downmixed and synchronously sampled via two National Instruments® universal software radio peripherals (USRPs). These front-ends fed their data to a Generalized Radionavigation Interfusion Device (GRID) software receiver [17], which produced pseudorange observables from five GPS L1 C/A signals in view, and the three cellular BTSs. Fig. 2 depicts the experimental hardware setup.

The pseudoranges were drawn from a receiver located at $\boldsymbol{r}_r = (10^6) \cdot [-2.430701, -4.697498, 3.553099]^{\mathsf{T}}$, expressed in an ECEF frame, which was surveyed using a Trimble 5700 carrier-phase differential GPS receiver. The corresponding SOP state estimates $\{\hat{\boldsymbol{x}}_{\mathsf{sop}_n}\}_{n=1}^{N}$, were collaboratively estimated by receivers in the navigating receiver's vicinity. The pseudoranges and SOP estimates were fed to a least-squares estimator, producing $\hat{\boldsymbol{x}}_r$ and associated $\mathbf{P}_{\tilde{\boldsymbol{x}}_r\tilde{\boldsymbol{x}}_r}$, from which the VDOP, HDOP, and GDOP were calculated and tabulated in Table II for M GPS SVs and N cellular CDMA SOPs. A sky plot of the GPS SVs used is shown in Fig. 4. The tower locations, receiver location, and a comparison of the resulting 95$^{\mathsf{th}}$-percentile estimation uncertainty ellipsoids of $\hat{\boldsymbol{x}}_r$ for $\{M, N\} = \{5, 0\}$ and $\{5, 3\}$ are illustrated in Fig. 3. The corresponding vertical error was 1.82m and 0.65m respectively. Hence, adding three SOPs to the navigation solution that used five GPS SVs reduced the vertical error by 64.5%. Although this is a significant improvement over using GPS observables alone, improvements for aerial vehicles are expected to be even more significant, since they can exploit a full span of observable elevation angles.

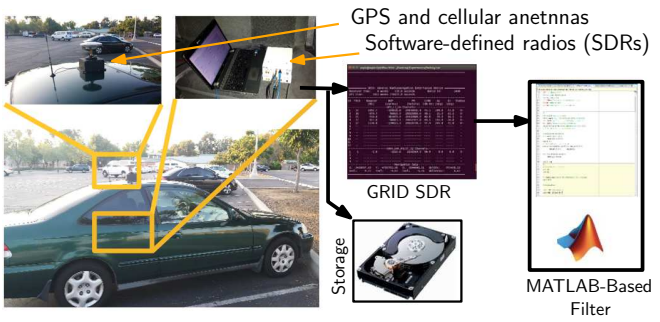

Fig. 2. Experiment hardware setup

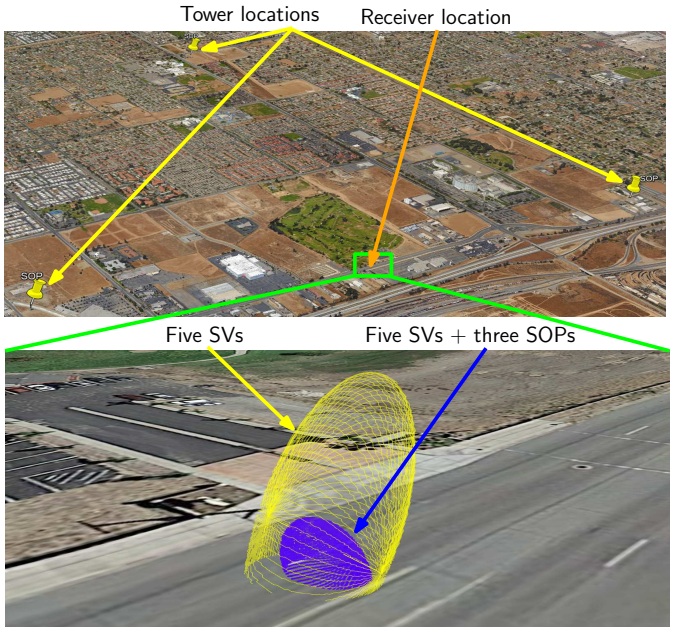

Fig. 3. Top: Cellular CDMA SOP tower locations and receiver location. Bottom: uncertainty ellipsoid (yellow) of navigation solution from using pseudoranges from five GPS SVs and uncertainty ellipsoid (blue) of navigation solution from using pseudoranges from five GPS SVs and three cellular CDMA SOPs.

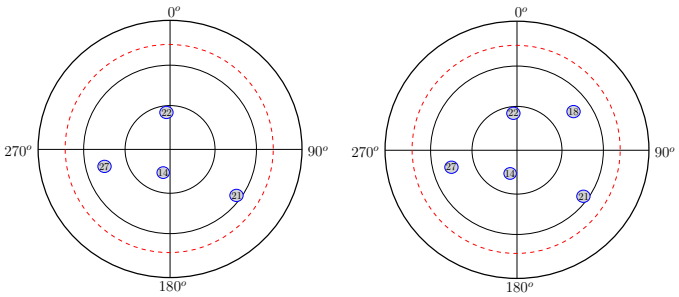

Fig. 4. Left: Sky plot of GPS SVs: 14, 21, 22, and 27 used for the four SV scenarios. Right: Sky plot of GPS SVs: 14, 18, 21, 22, and 27 used for the five SV scenarios. The elevation mask, $el_{\mathsf{sv,min}}$, was set to 20° (dashed red circle).

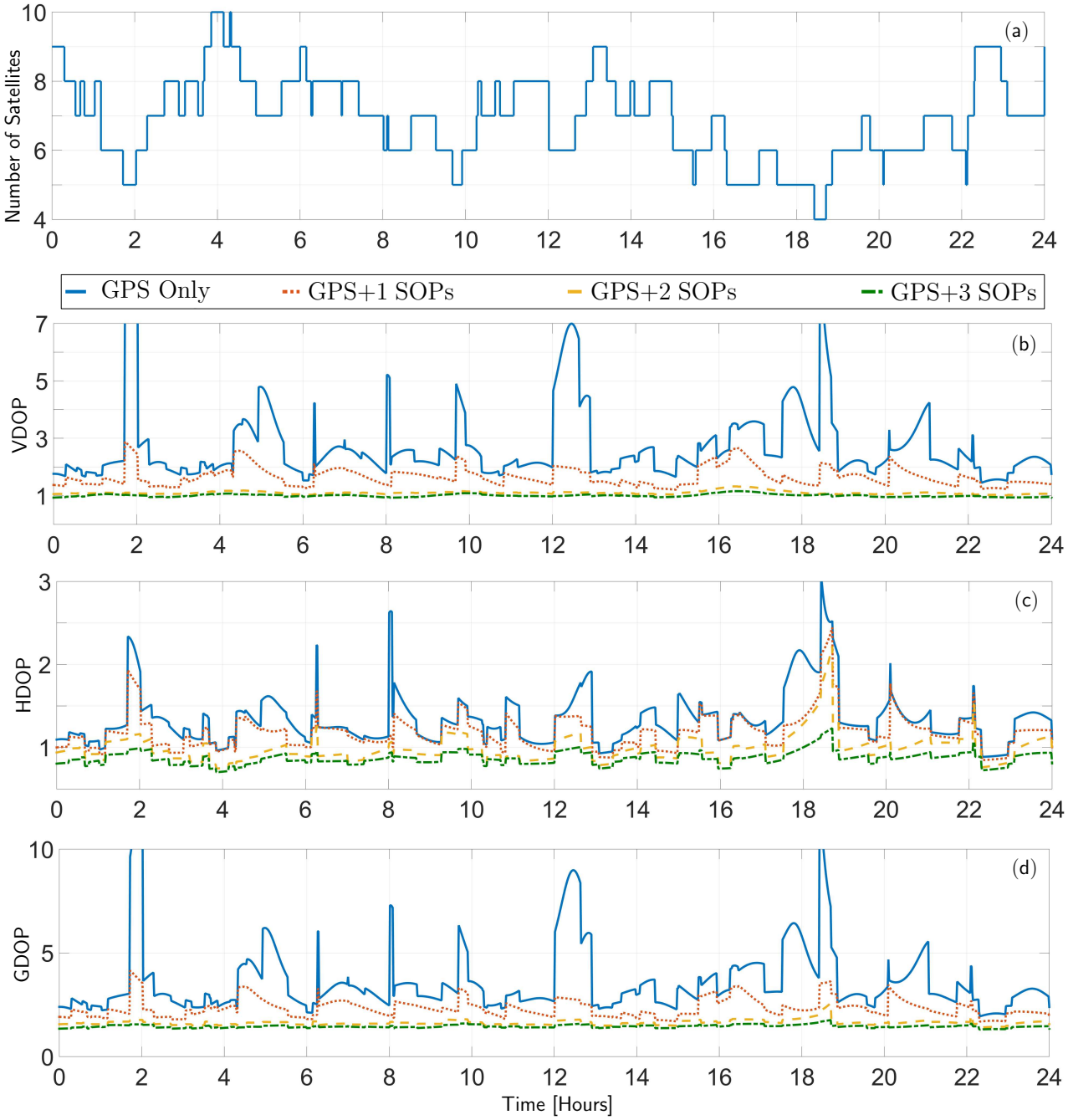

Fig. 5. Fig. (a) represents the number of SVs with an elevation angle $> 20°$ as a function of time. Fig. (b)–(d) correspond to the resulting VDOP, HDOP, and GDOP, respectively, of the navigation solution using GPS only, GPS + 1 SOP, GPS + 2 SOPs, and GPS + 3 SOPs.

TABLE II
DOP VALUES FOR M SVS + N SOPS

(M) **SVs,** (N) **SOPs:** $\{M, N\}$	**{4, 0}**	**{4, 1}**	**{4, 2}**	**{4, 3}**	**{5, 0}**	**{5, 1}**	**{5, 2}**	**{5, 3}**
VDOP	3.773	1.561	1.261	1.080	3.330	1.495	1.241	1.013
HDOP	2.246	1.823	1.120	1.073	1.702	1.381	1.135	1.007
GDOP	5.393	2.696	1.933	1.654	4.565	2.294	1.880	1.566

VI. CONCLUSIONS

This paper studied the reduction of VDOP of a GNSS-based navigation solution by exploiting terrestrial SOPs. It was demonstrated that the VDOP of GNSS solution can be reduced by exploiting the inherently small elevation angles of terrestrial SOPs. Experimental results using ground vehicles equipped with SDRs demonstrated VDOP reduction of a GNSS navigation solution by exploiting a varying number of cellular CDMA SOPs. Incorporating terrestrial SOP observables alongside GNSS SV observables for VDOP reduction is particularly attractive for aerial systems, since a full span of observable elevation angles become available.

References

[1] J. Raquet and R. Martin, "Non-GNSS radio frequency navigation," in *Proceedings of IEEE International Conference on Acoustics, Speech and Signal Processing*, March 2008, pp. 5308–5311.

[2] K. Pesyna, Z. Kassas, J. Bhatti, and T. Humphreys, "Tightly-coupled opportunistic navigation for deep urban and indoor positioning," in *Proceedings of ION GNSS Conference*, September 2011, pp. 3605–3617.

[3] Z. Kassas, "Collaborative opportunistic navigation," *IEEE Aerospace and Electronic Systems Magazine*, vol. 28, no. 6, pp. 38–41, 2013.

[4] P. Massat and K. Rudnick, "Geometric formulas for dilution of precision calculations," *NAVIGATION, Journal of the Institute of Navigation*, vol. 37, no. 4, pp. 379–391, 1990.

[5] N. Levanon, "Lowest GDOP in 2-D scenarios," *IEE Proceedings Radar, Sonar and Navigation*, vol. 147, no. 3, pp. 149–155, 2000.

[6] I. Sharp, K. Yu, and Y. Guo, "GDOP analysis for positioning system design," *IEEE Transactions on Vehicular Technology*, vol. 58, no. 7, pp. 3371–3382, 2009.

[7] N. Blanco-Delgado and F. Nunes, "Satellite selection method for multi-constellation GNSS using convex geometry," *IEEE Transactions on Vehicular Technology*, vol. 59, no. 9, pp. 4289–4297, November 2010.

[8] P. Misra and P. Enge, *Global Positioning System: Signals, Measurements, and Performance*, 2nd ed. Ganga-Jamuna Press, 2010.

[9] M. K. J. Barnes, C. Rizos and A. Pahwa, "A soultion to tough GNSS land applications using terrestrial-based transciers (LocataLites)," in *Proceedings of ION GNSS Conference*, September 2006, pp. 1487–1493.

[10] Z. Kassas, V. Ghadiok, and T. Humphreys, "Adaptive estimation of signals of opportunity," in *Proceedings of ION GNSS Conference*, September 2014, pp. 1679–1689.

[11] J. Morales and Z. Kassas, "Optimal receiver placement for collaborative mapping of signals of opportunity," in *Proceedings of ION GNSS Conference*, September 2015, pp. 2362–2368.

[12] Z. Kassas and T. Humphreys, "Observability analysis of collaborative opportunistic navigation with pseudorange measurements," *IEEE Transactions on Intelligent Transportation Systems*, vol. 15, no. 1, pp. 260–273, February 2014.

[13] J. Spilker, Jr., *Global Positioning System: Theory and Applications*. Washington, D.C.: American Institute of Aeronautics and Astronautics, 1996, ch. 5: Satellite Constellation and Geometric Dilution of Precision, pp. 177–208.

[14] D. H. Won, J. Ahn, S. Lee, J. Lee, S. Sung, H. Park, J. Park, and Y. J. Lee, "Weighted DOP with consideration on elevation-dependent range errors of GNSS satellites," *IEEE Transactions on Instrumentation and Measurement*, vol. 61, no. 12, pp. 3241–3250, December 2012.

[15] Federal Communications Commission, "Overview of small UAS notice of proposed rulemaking," https://www.faa.gov/uas/nprm/, February 2015, accessed November 25, 2015.

[16] University of California, San Diego, "Garner GPS archive," http://garner.ucsd.edu/, accessed November 23, 2015.

[17] T. Humphreys, J. Bhatti, T. Pany, B. Ledvina, and B. O'Hanlon, "Exploiting multicore technology in software-defined GNSS receivers," in *Proceedings of ION GNSS Conference*, September 2009, pp. 326–338.